Direct Dynamics Study of Intramolecular Proton Transfer in Hydrogenoxalate Anion

Thanh N. Truong* and J. Andrew McCammon

Contribution from the Department of Chemistry, University of Houston, Houston, Texas 77204.
Received February 20, 1991

Abstract: We have carried out ab initio calculations for the intramolecular proton-transfer process in hydrogenoxalate anion using Møller–Plesset perturbation theory with a reasonably large basis set. We found that electron correlation is very important in predicting the barrier height as well as the equilibrium and transition-state structures. The classical barrier height calculated at the MP2/6-31++G** level is 3.1 kcal/mol. Including the zero-point energy correction reduces the barrier to only 0.4 kcal/mol for the proton transfer, and to 1.3 and 1.6 kcal/mol for the deuterium and tritium isotope substituted reactions, respectively. We also used these results with transition-state theory and an Eckart semiclassical tunneling method to calculate the rate constants and kinetic isotope effect for this reaction. We found that the tunneling contribution to the rate constant is smaller for the proton transfer than for other heavier isotopes. The calculated kinetic isotope effect is quite large and due mostly to the in-plane hydrogen stretch and bend vibrational modes.

1. Introduction

Proton transfer is one of the most important processes in biological systems, especially in enzyme catalysis reactions.[1-5] Due to the small transferring mass, quantum mechanical tunneling is expected to be prominent in such processes.[2-5] Recent experimental studies have found that the kinetic isotope effect (KIE) for proton transfer in enzyme reactions can be quite large and have attributed this to quantum mechanical tunneling.[5] Unfortunately, theoretical investigations so far have been limited to small model reactions and yet still suffered limitations in dynamical calculations of reaction rates and KIE.[6-8] One of the most severe limitations is that most of the dynamical methods are based on semiempirical analytical potential energy functions. The development of such potential energy functions is not a simple task, and their adequacy depends on the developer's preconceived notions of their correct functional forms. Such limitations have encouraged much effort in developing direct dynamics methods that can calculate dynamical observable quantities directly from electronic structure information without the need of an analytical potential energy function.[9-11]

Recent developments in this area have led to two different approaches[12-14] resulting from compromises between the accuracy of the electronic structure calculations and the adequacy of the dynamical methods. When it is impractical to carry out full electronic structure calculations for all the data needed to perform the full dynamics calculation, one can employ an accurate electronic structure method only for a small set of points and use approximate dynamical methods such as interpolated variational transition-state theory[12,13] (IVTST) to estimate the rate constants. For systems with large tunneling, one would employ the other approach, that is, to carry out full variational transition-state theory[14] calculations with the large-curvature tunneling method[15] at a less accurate electronic structure level, e.g., using semiempirical molecular orbital methods.[16] To offset the deficiency of the semiempirical MO methods, one can adjust their parameters for a specific reaction; in other words, one uses the semiempirical MO Hamiltonian entirely as a fitting function.[17] These two approaches have shown considerable promise.

In the present study, we have considered the intramolecular proton transfer in hydrogenoxalate anion.

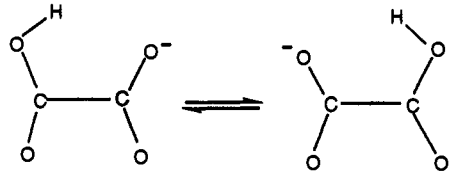

We have carried out rather extensive ab initio calculations, and the results are used to estimate the gas-phase transfer rate constant and the KIE using the lowest order of the interpolated variational transition-state theory (IVTST), that is, the transition-state theory plus the semiclassical zero-curvature ground-state tunneling method.[12] The reason for using this dynamical model will become apparent later.

The present study has several objectives. Firstly, it serves as a model study for proton transfer in many enzymatic reactions, though it also poses important questions in its own right. Here, we are particularly interested in the quantum mechanical effects, namely, zero-point energy motions and tunneling, on the experimentally observable quantities such as the transfer rate and KIE. Secondly, it provides a test for the employed dynamical model. Finally, the present study can be used as a reference point for the ongoing effort in our research group to develop a time-dependent dynamical method for studying processes in which only a few degrees of freedom require the full quantum mechanical treatment while the remaining ones can be treated classically, such as proton transfer in protein or in solution. However, it is important to point out that the present study is done for the gas-phase reaction. In

(1) Page, M. T. *The Chemistry of Enzyme Action*; Elsevier: Amsterdam, 1974.
(2) Caldin, E. F., Gold, V., Eds. *Proton-transfer Reactions*; Chapman & Hall: London, 1975.
(3) Bell, R. P. *The Tunnel Effect in Chemistry*; Chapman & Hall: London, 1980.
(4) Borgis, D.; Hynes, J. T. In *The Enzyme Catalysis Process*, Cooper, A., Houben, J., Chien, L., Eds.; Plenum: New York, 1989.
(5) Cha, Y.; Murray, C. J.; Klinman, J. P. *Science* **1989**, *243*, 1325.
(6) Esquivel, J. L.; Mata-Segreda, J. F. *Int. J. Quantum Chem.* **1990**, *38*, 521.
(7) Bosch, E.; Moreno, M.; Lluch, J. M.; Bertran, J. *J. Chem. Phys.* **1990**, *93*, 5685.
(8) Wolfe, S.; Hoz, S.; Kim, C.; Yang, K. *J. Am. Chem. Soc.* **1990**, *112*, 4186.
(9) Warshel, A.; Weiss, R. M. *J. Am. Chem. Soc.* **1980**, *102*, 6218. Warshel, A.; Russell, S. T. *Q. Rev. Biophys.* **1984**, *17*, 283.
(10) Singh, U. C.; Kollman, P. A. *J. Comput. Chem.* **1986**, *7*, 718.
(11) Bash, P. A.; Field, M. J.; Karplus, M. *J. Am. Chem. Soc.* **1987**, *109*, 8092. Field, M.-J.; Bash, P. A.; Karplus, M. *J. Comput. Chem.* **1990**, *11*, 700.
(12) Truong, T. N.; Truhlar, D. G. *J. Chem. Phys.* **1990**, *93*, 1761.
(13) Gonzalez-Lafont, A.; Truong, T. N.; Truhlar, D. G. To be published.
(14) Truhlar, D. G.; Isaacson, A. D.; Garrett, B. C. In *The Theory of Chemical Reaction Dynamics*; Baer, M., Ed.; CRC Press: Boca Raton, FL, 1985; p 65.
(15) Garrett, B. C.; Joseph, T.; Truong, T. N.; Truhlar, D. G. *Chem. Phys.* **1989**, *136*, 271.
(16) Pople, J. A.; Beveridge, D. L. *Approximate Molecular Orbital Theory*; McGraw-Hill: New York, 1970.
(17) Gonzalez-Lafont, A.; Truong, T. N.; Truhlar, D. G. *J. Phys. Chem.*, in press.

0002-7863/91/1513-7504$02.50/0

the condensed phase, the coupling between the environment and the proton motions is often strong. It changes both the barrier and the shape of the double minimum potential of proton transfer, and thus, it would result in a different KIE.[4] Such solvent effects are under consideration in the development of the dynamical method mentioned above.

In the next section, we present the computational methodology of both the electronic structure and dynamical calculations. The results and discussion are given in section 3.

2. Computational Methodology

The computational procedure consists of two stages. In the first stage, ab initio calculations are carried out by using the GAUSSIAN88 program[18] employing moderate-size split-valence basis sets, in particular, the 6-31+G* basis in which sets of d orbitals and sp diffuse functions are added to heavy atoms C and O, and the 6-31++G** basis, which is the same as the 6-31+G* basis except an additional diffuse s orbital and a set of p orbitals are added to the hydrogen atom.

In all these ab initio calculations, electrons are restricted to doubly occupied orbitals. The geometries at the reactant and transition state are fully optimized at the Hartree–Fock (HF) level using both basis sets, and at the second-order Møller-Plesset (MP2) many-body perturbation theory[19] level using the 6-31++G** basis set, and also using C_s symmetry for the reactant and C_{2v} symmetry for the transition state. The force constant calculations at the HF/6-31++G** level in fact confirm the symmetrical nature of these critical points; i.e., the force constant matrix has no negative eigenvalue for the equilibrium structure, and has only one negative eigenvalue for the transition state. Electron correlation is included in the MP2 calculations.

In the second stage, the rate constant at temperature T for the intramolecular proton transfer in the hydrogenoxalate anion is calculated from

$$k(T) = \kappa k^{TST}(T) \tag{1}$$

where k^{TST} is the transition state theory rate constant, which can be expressed as[20]

$$k^{TST} = \frac{1}{\beta h}\frac{Q^{\ddagger}}{Q_R}e^{-\beta\Delta V^{\ddagger}} \tag{2}$$

h is the Planck constant; β is $(k_B T)^{-1}$, where k_B denotes the Boltzmann constant. $Q^{\ddagger}$ and Q_R are the transition-state and reactant partition functions, respectively, which are products of the electronic, rotational, and vibrational partition functions. Note that, for unimolecular processes, the translational partition functions for the transition state and reactant cancel. The rotational partition functions, which depend on the geometries, are calculated classically, and the geometries of the reactant and transition state are taken from MP2/6-31++G** calculations. The vibrational partition functions are computed quantum mechanically by using the harmonic approximation, and the frequencies are taken from HF/6-31++G** calculations. $\Delta V^{\ddagger}$ is the classical barrier height with the value taken from the most accurate calculation in the present study, namely, MP2/6-31++G** level. The transmission coefficient, κ, accounts for the quantum mechanical tunneling in the direction along the reaction coordinate and is calculated by the semiclassical zero-curvature ground-state (ZCG) method. The mathematical details of this Eckart model for tunneling calculations are given in a previous study[12] by one of us. In this method, the proton is restricted to tunnel along the minimum energy path and the bound motions are assumed to adjust adiabatically to their ground states. The adiabatic ground-state potential along the minimum energy path is then modeled by an Eckart function that gives correct results at the reactant, product, and transition state, and has the same width as the classical potential along the minimum energy path. In a previous work,[12] the ZCG method has shown a significant improvement over the Wigner correction in estimating the tunneling transmission coefficient for hydrogen atom transfer reaction. Note that the transmission coefficients defined here neglect effects other than tunneling (e.g., over barrier recrossing, nonadiabatic effects...). These other effects are discussed in the next section.

Table I. Energy (au) and Equilibrium Geometry of Hydrogenoxalate Anion (Bond Length, Å; Angle, deg)

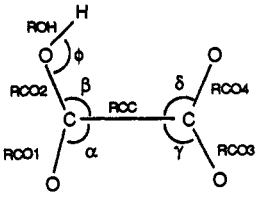

variables	HF 3-21+G[a]	HF 6-31+G*	HF 6-31++G**	MP2 6-31++G**
R(CC)	1.57	1.578	1.577	1.575
R(CO1)	1.21	1.118	1.118	1.221
R(CO2)	1.36	1.330	1.329	1.358
R(CO3)	1.24	1.214	1.214	1.246
R(CO4)	1.27	1.243	1.243	1.283
R(OH)	0.98	0.962	0.958	1.001
α	127.4	126.8	126.8	127.6
β	110.7	111.5	111.3	109.8
γ	117.9	117.1	117.1	118.2
δ	110.9	111.4	111.3	110.9
ϕ	107.7	104.4	104.2	98.9
E		−375.855 341	−375.862 049	−376.875 960

[a] Results are taken from ref 21.

Table II. Energy (au) and Geometry of the Intramolecular Proton-Transfer Transition State in Hydrogenoxalate Anion (Bond Length, Å; Angle, deg)

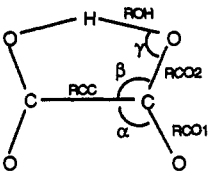

variables	HF 3-21+G[a]	HF 6-31+G*	HF 6-31++G**	MP2 6-31++G**
R(CC)	1.58	1.574	1.573	1.574
R(CO1)	1.22	1.199	1.199	1.233
R(CO2)	1.32	1.283	1.283	1.317
R(OH)	1.23	1.207	1.201	1.224
α	125.0	124.8	124.9	124.7
β	105.8	106.0	105.9	106.8
γ	95.6	93.0	92.7	91.1
E		−375.838 513	−375.847 299	−376.871 029

[a] Results are taken from ref 21.

The results from both ab initio and dynamical calculations are given in the next section.

3. Results and Discussion

3.1. Statics. The optimized geometries of the equilibrium structure and transition state are given in Tables I and II. As mentioned earlier, the force constant calculations confirm that the equilibrium structure has C_s symmetry and the transition state has C_{2v} symmetry. Comparing to the previous calculations of Bosh et al.,[21] we found that adding d orbitals to both C and O atoms at HF/6-31+G* significantly decreases the C–O and O–H bond lengths of both the equilibrium structure and transition state by 0.02–0.04 Å. The angle H–O–C is also decreased in both structures by about 3°. There is little effect on the structure at the HF level by adding diffuse s and p orbitals to the hydrogen atom. However, electron correlation from these additional diffuse and polarization orbitals on all atoms has a profound effect on the structure. Geometry optimization at MP2/6-31++G** shows that the C–O bonds of both equilibrium and transition-state structures are elongated by 0.02–0.03 Å compared to HF results.

(18) Frisch, M. J.; Head-Gordon, M.; Schlegel, H. B.; Raghavachari, K.; Binkley, J. S.; Gonzalez, C.; Defrees, D. J.; Fox, D. J.; Whiteside, R. A.; Seeger, R.; Melius, C. F.; Baker, J.; Martin, R. L.; Kahn, L. R.; Stewart, J. J. P.; Fluder, E. M.; Topiol, S.; Pople, J. A. *GAUSSIAN88*; Gaussian, Inc.: Pittsburgh, PA.

(19) Hehre, W. J.; Radom, L.; Schleyer, P. R.; Pople, J. A. *Ab Initio Molecular Orbital Theory*; Wiley: New York, 1986.

(20) Glasstone, S.; Laidler, K. J.; Eyring, H. *Theory of Rate Processes*; McGraw-Hill: New York, 1941.

(21) Bosch, E.; Moreno, M.; Lluch, J. M.; Bertran, J. *Chem. Phys.* **1990**, *148*, 77.

Table III. Reactant and Transition-State Frequencies (cm^{-1}) Calculated at HF/6-31++G**

	reactant			transition state		
mode	H	D	T	H	D	T
1	84 (a'')	84	84	1649i (b2)	1206i	1008i
2	329 (a')	321	313	146 (a2)	146	146
3	467 (a')	453	441	369 (a1)	369	369
4	555 (a'')	551	524	555 (b1)	553	550
5	604 (a')	597	589	658 (b2)	657	655
6	774 (a')	763	751	791 (a1)	791	791
7	880 (a'')	644	569	822 (b2)	822	822
8	921 (a')	917	908	941 (a2)	941	941
9	939 (a'')	939	939	969 (a1)	969	969
10	1279 (a')	1087	973	1400 (b1)	1014	849
11	1491 (a')	1370	1357	1436 (b2)	1418	1408
12	1551 (a')	1525	1524	1497 (a1)	1455	1535
13	1916 (a')	1915	1914	1951 (a1)	1630	1277
14	2027 (a')	2017	2015	1982 (b2)	1969	1964
15	3913 (a')	2847	2393	2287 (a1)	2005	1955
ZPE[a]	25.35	22.91	21.86	22.59	21.07	20.40

[a] Harmonic zero-point energy (kcal/mol).

Table IV. Calculated Barrier Height (kcal/mol) for the Intramolecular Proton Transfer in Hydrogenoxalate Anion

level/basis	$\Delta V^{\ddagger}$	
HF/3-21+G	8.3[a]	
HF/6-31+G//3-21+G	12.6[a]	
HF/6-31+G*	10.6	
HF/6-31++G**	9.3	
MP2/6-31+G//3-21+G	10.6[a]	
MP2//6-31+G*	3.9	
MP2//6-31++G**	2.6	
MP2/6-31++G**	3.1[b]	$(0.4)_H$[c]
		$(1.3)_D$
		$(1.6)_T$

[a] Results are taken from ref 21. [b] Best value. [c] Zero-point energy corrections calculated at HF/6-31++G** are added for different isotopes.

The O–H bonds from both structures are also stretched somewhat.

The vibrational frequencies of the hydrogenoxalate anion and the transition state for the intramolecular proton transfer are listed in Table III, along with the corresponding deuterium- and tritium-substituted results. Due to a large difference in the geometries calculated at the HF and MP2 levels, one would expect the calculated frequencies to be different at these levels. Although it is more desirable to calculate these frequencies at the MP2 level of theory since they will be used later in the rate calculations, computationally it is not feasible in the present study. Notice that the differences in the frequency between isotopes for both the reactant and transition state are mostly localized to a few vibrational modes which have a large hydrogenic characteristic. These vibrational modes in fact have a profound effect on the KIE for the proton-transfer process as will be discussed in the next subsection.

The classical barrier heights for the intramolecular proton transfer in hydrogenoxalate anion obtained from different levels of calculations are listed in Table IV. First notice that the HF results for the barrier vary with different basis sets; however, the barrier is not increasing with the size of the basis set as has been observed in the previous study.[21] In particular, adding d orbitals to C and O atoms as in the 6-31+G* basis set raises the barrier by 2.3 kcal/mol compared to the 3-21+G result from the Bosh et al. calculations,[21] but adding diffuse s and p orbitals to hydrogen as in the 6-31++G** basis set then lowers the HF barrier by 1.3 kcal/cal. The HF barrier calculated at the largest basis set in this study is 9.3 kcal/mol.

For moderate size systems such as the one considered here, the electron correlation contribution is commonly estimated by single-point many-body perturbation theory calculations at HF-optimized geometries. The use of HF structures in MP calculations assumes that the HF-optimized structures at the stationary points are not too different from those of MP calculations. A previous study[22] shows that this assumption is often not satisfied and the results sometimes are not correct. In the present work, as shown in Table IV, the single-point MP2 calculations yield barrier heights varying from 10.6 to 2.6 kcal/mol. The results clearly indicate that d and p polarization orbitals are quite important at the correlated level of theory. Due to the importance of the barrier in the later dynamical calculations, we have optimized the reactant and transition-state structures at the MP2/6-31++G** level, and found the classical barrier height to be 3.1 kcal/mol. Adding the zero-point energy correction calculated at HF/6-31++G** lowers the barrier to 0.4 kcal/mol for the proton transfer, and to 1.3 and 1.6 kcal/mol for the deuteron and triton transfer, respectively. It would be preferable to use the barrier and frequencies calculated at the same level of theory, namely, MP2/6-31++G** in this case, in calculating the zero-point energy correction and rate constants. The HF barrier is too high compared to the more accurate MP2 one; thus, it would result in much smaller rate constants and larger tunneling contributions, whereas to obtain MP2 frequencies for this system requires a large computer resource even on the CRAY-YMP. However, due to the independent normal mode approximation within the reaction path Hamiltonian framework, one can scale the potential energy along the reaction coordinate without affecting the eigenvalues of the modes perpendicular to it. The eigenvalue of the mode along the reaction coordinate, i.e., the imaginary frequencies at the transition state in the TST theory, on the other hand would be affected. In the present work, the imaginary frequency is used in the Eckart model to estimate the tunneling contribution. Since the effective barriers are small, we expect tunneling will also be small; thus, the effect on the imaginary frequency would not affect the final results significantly. Therefore, we believe that using the more accurate MP2 barrier in conjunction with the HF frequencies still gives a valid qualitative picture of the dynamics of this system. Furthermore, since the tunneling is expected to be small, we believe that the zero-curvature ground-state tunneling method in conjunction with transition-state theory is adequate for our objectives.

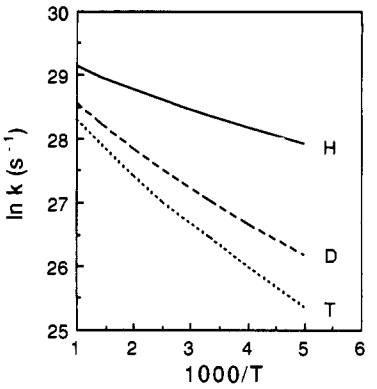

Figure 1. Natural logarithmic plot of rate constants (s^{-1}) versus $1000/T$ for the intramolecular proton transfer in hydrogenoxalate anions and its deuterium- and tritium-substituted isotopes.

3.2. Dynamics. The TST and TST/ZCG rate constants for the proton transfer in hydrogenoxalate anion and for its corresponding deuterium- and tritium-substituted processes are given in Table V. Recall that TST rate constants do not include tunneling, though all vibrational degrees of freedom are treated quantum mechanically. Tunneling is included in TST/ZCG rate constants. The natural logarithmic plot of the final rate constants versus the inverse temperature is also shown in Figure 1. Notice that there is a large difference between the transfer rate of proton and its heavier isotopes especially at low temperatures, indicating that the KIE is substantial. The calculated KIE, in particular, the ratios of k_H/k_T and k_D/k_T, is listed in Table VI.

It is a common view that a large KIE is due mostly to quantum mechanical tunneling effects; i.e., a proton has smaller mass than a deuteron or triton; thus, it tunnels faster and has higher tunneling

(22) Truong, T. N.; Truhlar, D. G.; Baldridge, K. K.; Gordon, M. S.; Steckler, R. *J. Chem. Phys.* **1989**, *90*, 7137.

Table V. Calculated Rate Constants (s^{-1}) for the Intramolecular Proton Transfer in Hydrogenoxalate Anion

	H		D		T	
T (K)	TST	TST/ZCG	TST	TST/ZCG	TST	TST/ZCG
200	1.11 (12)[a]	1.32 (12)	1.11 (11)	2.30 (11)	4.75 (10)	1.02 (11)
250	1.52 (12)	1.70 (12)	2.35 (11)	3.79 (11)	1.17 (11)	1.92 (11)
300	1.89 (12)	2.05 (12)	3.91 (11)	5.46 (11)	2.15 (11)	3.03 (11)
350	2.23 (12)	2.36 (12)	5.61 (11)	7.19 (11)	3.30 (11)	4.25 (11)
400	2.52 (12)	2.63 (12)	7.37 (11)	8.92 (11)	4.56 (11)	5.34 (11)
500	3.01 (12)	3.10 (12)	1.08 (12)	1.22 (12)	7.18 (11)	8.13 (11)
700	3.73 (12)	3.78 (12)	1.69 (12)	1.81 (12)	1.12 (12)	1.31 (12)
1000	4.47 (12)	4.51 (12)	2.44 (12)	2.51 (12)	1.89 (12)	1.95 (12)

[a] Power of 10 in parentheses.

Table VI. Kinetic Isotope Effect for the Intramolecular Proton Transfer in Hydrogenoxalate Anion

	k_H/k_T		k_D/k_T		$(k_D/k_T)^{3.26}$
T (K)	TST	TST/ZCG	TST	TST/ZCG	TST
200	23.38	12.93	2.33	2.26	15.76
250	12.94	8.84	2.01	1.98	9.74
300	8.82	6.76	1.82	1.81	7.04
350	6.74	5.54	1.70	1.69	5.64
400	5.52	4.76	1.62	1.61	4.82
500	4.19	3.81	1.50	1.50	3.75
700	3.04	2.89	1.38	1.38	2.86
1000	2.37	2.32	1.29	1.29	2.29

probability; consequently it raises the KIE. However, in the ZCG method, aside from the transfer mass, the tunneling probability also depends on the length of the tunneling path and the adiabatic ground-state potential along this path. As shown in Table V, the tunneling contribution to the proton-transfer rate is smaller than those of deuteron and triton transfer. In particular, at 300 K, quantum mechanical tunneling enhances the transfer rate by 5% for proton, 40% for deuteron, and 41% for triton. The results in fact are not surprising, since the effective barrier is only 0.4 kcal/mol for proton transfer while it is 1.3 and 1.6 kcal/mol for deuteron and triton transfer, respectively. Thus, at room temperature, most of the proton trajectories starting at the reactant would have sufficient energy to surmount the barrier, while a larger portion of deuteron and triton trajectories would not, and hence the deuteron and triton have larger tunneling contributions to the transfer rate. Nevertheless, the overall transfer rate of deuteron and triton are still smaller. The tunneling effect in the present case therefore lowers the KIE. However, in the case of a large effective barrier where tunneling can enhance the transfer rate by several orders of magnitude, the calculated KIE may result almost entirely from tunneling. In this case, tunneling would increase the KIE.

Despite the fact that tunneling lowers the KIE, the final calculated KIE is still quite large. In particular, the k_H/k_T ratios vary from 2.32 to 12.93 as the temperature decreases from 1000 to 200 K. From the TST results for k_H/k_T, we can conclude that the large KIE for the intramolecular proton transfer in hydrogenoxalate anion is due to the quantal effect from the vibrational motions. In other words, the large difference in the zero-point energy (ZPE) between the hydrogen- and tritiumoxalate anions is only partly overcome by a small difference in ZPE at the transition states, which results in a large difference in the effective barrier for the two isotopes. Our present results are consistent with the previous finding of the "anomalous" KIE in other proton-transfer reactions.[8]

It is worthwhile to compare our present results for the KIE with those calculated from a semiclassical model.[23,24] This model gives a relation between the two isotope effects k_H/k_T and k_D/k_T that can be expressed as

$$\frac{k_H}{k_T} = \left(\frac{k_D}{k_T}\right)^{3.26} \tag{3}$$

This relation was derived strictly from zero-point energy motions; thus, it was used as a test for quantum mechanical tunneling in many experimental studies.[5,25] That is, if tunneling is significant, then the observed k_H/k_T would be distinctly larger than that calculated from eq 3. The k_H/k_T ratios calculated by eq 3 using TST results for k_D/k_T are listed in the last column of Table VI. Notice that these ratios are noticeably smaller than the exact (no tunneling) TST results; thus, we caution against the use of the above relation. The difference here is due mainly to the fact that this model does not account for the distribution of molecules in higher vibrational states in both the reactant and transition state.

For further analysis of the KIE, we factor the KIE into contributions from different types of motions. To accomplish this, we first assume that there is no coupling between electronic, vibrational, and rotational energies, and that the electronic partition functions for the reactant and transition state cancel in the kinetic isotope effect.[26] Furthermore, within the TST framework, there is no contribution to the KIE from the potential energy. The ratios k_H/k_T can be factorized as

$$\frac{k_H}{k_T} = \eta = \eta_{tun}\eta_{rot}\eta_{vib} \tag{4}$$

where

$$\eta_{tun} = \frac{\kappa_H}{\kappa_T} \tag{5}$$

$$\eta_{rot} = \frac{Q^{\ddagger}_{rot,H}Q^{R}_{rot,T}}{Q^{R}_{rot,H}Q^{\ddagger}_{rot,T}} \tag{6}$$

and

$$\eta_{vib} = \frac{Q^{\ddagger}_{vib,H}Q^{R}_{vib,T}}{Q^{R}_{vib,H}Q^{\ddagger}_{vib,T}} \tag{7}$$

κ_H and κ_T are the transmission coefficients for the proton and triton transfer, respectively. $Q^{\ddagger}_{rot,X}$ and $Q^{R}_{rot,X}$ are the transition state and reactant rotational partition functions for X (H or T) transfer reactions, respectively, and similarly for the vibrational partition functions, $Q^{\ddagger}_{vib,X}$ and $Q^{R}_{vib,X}$.

In order to analyze the relative importance of different vibrational modes, the vibrational contribution, η_{vib}, is further factorized as the product of three components, $\eta_{vib,in}$, $\eta_{vib,out}$, and $\eta_{vib,bb}$.

$$\eta_{vib} = \eta_{vib,in}\eta_{vib,out}\eta_{vib,bb} \tag{8}$$

$\eta_{vib,in}$ is the contribution from the in-plane vibrational modes that have the large H (or T) motions. From Table III, these are mode number 10, 11, and 15 for the reactant, and mode number 12, 13, and 15 for the transition state. Similarly, $\eta_{vib,out}$ is from the out-of-plane hydrogenic bend mode, which is mode 7 at the reactant, and mode 10 at the transition state. $\eta_{vib,bb}$ is the contribution from the remaining vibrational modes, which consist of

(23) Swain, C. J.; Stivers, E. C.; Reuwer, J. F., Jr.; Schaad, L. J. *J. Am. Chem. Soc.* **1958**, *80*, 5885.
(24) Saunders, W. H., Jr. *J. Am. Chem. Soc.* **1985**, *107*, 164.
(25) Melander, L.; Saunders, W. H., Jr. *Reaction Rates of Isotopic Molecules*; Wiley: New York, 1980.
(26) Tucker, S. C.; Truhlar, D. G.; Garrett, B. C.; Isaacson, A. D. *J. Chem. Phys.* **1985**, *82*, 4102.

Table VII. Contributions of Various Types of Motions to the Ratios k_H/k_T[a]

T (K)	η_{tun}	η_{rot}	$\eta_{vib,in}$	$\eta_{vib,out}$	$\eta_{vib,bb}$
200	0.55	1.01	35.44	0.42	1.54
300	0.77	1.01	10.85	0.58	1.38
500	0.91	1.01	4.26	0.75	1.30

[a] $\eta_{vib,in}$ is from in-plane hydrogenic stretch and bend vibrational modes. $\eta_{vib,out}$ is from the out-of-plane hydrogenic bend vibrational mode. $\eta_{vib,bb}$ is from the remaining backbone vibrational modes.

mostly the backbone heavy atom motions. These individual contributions can be calculated by using eq 7 for selected mode(s).

The resulting contributions to the ratios of k_H/k_T are given in Table VII. First of all, the rotational motions, as expected, have little effect on the KIE; i.e., η_{rot} is near unity for the entire temperature range. As discussed earlier, tunneling decreases the KIE; in particular, η_{tun} decreases from 0.91 to 0.55 as the temperature decreases from 500 to 200 K. For the vibrational motions, the out-of-plane hydrogenic bend mode is found to decrease the KIE. This is probably due to the fact the hydrogen out-of-plane bend mode is tighter at the transition state than at the reactant. Interestingly, we found that the hydrogenic in-plane modes are mostly responsible for the large KIE observed in this reaction. $\eta_{vib,in}$ increases from 4.26 to 35.44 as the temperature decreases from 500 to 200 K. The remaining backbone modes account for a 30–60% increase in the KIE for the temperature range from 200 to 500 K.

It is important to point out that there are some limitations in the present calculations. First of all, recrossing effects are not included in this study. Such effects would lower the calculated transfer rates, and might be important for double well potentials with low barriers such as those considered here. For proton transfer in the hydrogenoxalate anion, one might expect the recrossing effect to be larger for the proton than for its heavier isotopes, since it has the smallest effective barrier. Consequently, it would lower the calculated KIE somewhat. Finally, the anharmonicity effects were not included in calculating the vibrational partition functions and zero-point energies in the present calculations. Such effects might be nonnegligible for low-frequency modes.

4. Conclusion

We have carried out ab initio calculations for the intramolecular proton transfer in the hydrogenoxalate anion. We found that electron correlation, especially from d orbitals on the heavy atoms, is quite important in predicting the barrier height and the structures of both the reactant and transition state. The classical barrier height for this process calculated at the MP2/6-31++G** level is 3.1 kcal/mol as compared to the order of 9–10 kcal/mol at the HF level. Including the zero-point energy correction calculated at the HF/6-31++G** level reduces the barrier to only 0.4 kcal/mol for proton transfer, and to 1.3 and 1.6 kcal/mol for deuteron and triton transfer, respectively.

The rate constants and KIE for the intramolecular proton-transfer process are calculated by using transition-state theory plus the semiclassical zero-curvature ground-state tunneling method. Due to the small effective barrier, we found that the tunneling contribution to the rate constants is small for this proton-transfer reaction. Despite the effect of tunneling, the KIE is still anomalously large due mainly to the in-plane hydrogenic stretch and bend vibrational modes.

Acknowledgment. We are grateful to Professors Mark S. Gordon, Tom Albright, and Donald G. Truhlar for helpful discussions. This work has been supported in part by the National Science Foundation, the Robert A. Welch Foundation, the Texas Advanced Research Program, and the National Center for Supercomputing Applications. T.N.T. is the recipient of a National Science Foundation Postdoctoral Fellowship. J.A.M. is the recipient of the G. H. Hitchings Award from the Burroughs Wellcome Fund.

Vibrational Stabilization of Preferred Conformations of Partially Deuterated *n*-Butane Cations: Comparison of ab Initio Calculations and Electron Spin Resonance Results

S. Lunell,* L. A. Eriksson, and L. Worstbrock[†]

Contribution from the Department of Quantum Chemistry, Uppsala University, Box 518, S-751 20 Uppsala, Sweden. *Received May 11, 1990*

Abstract: The role of the zero-point vibrational energy (ZPE) in determining the preferred conformations of partially deuterated *n*-butane cations has been studied, using ab initio UHF/6-31G** and MP2/6-31G* calculations. By comparison with matrix isolation electron spin resonance (ESR) measurements, it is found that the experimental spectra at 77 K are fully explained by assuming a Boltzmann distribution over the nine possible rotational isomers related by rotations of the terminal methyl groups. The spectrum at 4 K, however, corresponds to the equilibrium distribution at a considerably higher temperature, 40–50 K, indicating that equilibration through rotational rearrangement is hindered at temperatures lower than this. In addition, hyperfine coupling constants, obtained from configuration interaction (SDCI) calculations, are reported and compared with experiment.

The use of selective deuteration in electron spin resonance (ESR) experiments has proven to be a powerful technique to investigate the structure of hydrocarbon radical cations, by distinguishing groups of chemically inequivalent protons.[1] Upon ionization, however, distortions often occur, which cause protons which are chemically equivalent in the un-ionized molecule to become structurally inequivalent in the cation. This is obvious

[†] Permanent address: Iwan Stranski Institute for Physical and Theoretical Chemistry, Technische Universität Berlin, Berlin, Germany.

(1) For a recent review, see: Shiotani, M.; Lund, A. In *Radical Ionic Systems*; Lund, A., Shiotani, M., Eds.; Kluwer Academic Publishers: Dordrecht, 1991; pp 151–176.

0002-7863/91/1513-7508$02.50/0